TEKTONIKA

Supporting Information

The Importance of Anisotropic Viscosity in Numerical Models for Olivine Textures in Shear and Subduction Deformations

TEKTONIKA 2024

Yijun Wang[1,2,*]
Ágnes Király[1,2]
Clinton P. Conrad[1,2]
Lars N. Hansen[3]
Menno Fraters[4]

[1] Centre for Planetary Habitability (PHAB), University of Oslo, Oslo, Norway
[2] Centre for Earth Evolution and Dynamics (CEED), University of Oslo, Oslo, Norway
[3] Department of Earth and Environmental Sciences, University of Minnesota, Minneapolis, MN, USA
[4] Department of Geological Sciences, University of Florida, Gainesville, FL, USA

** yijun0509wang@gmail.com*

Table of contents

1. Rheology parameters

We use a composite rheology where the dislocation and diffusion creep viscosity are computed separately using:

$$\eta_i = \frac{1}{2} A_i^{-\frac{1}{n_i}} d^{\frac{m_i}{n_i}} \dot{\varepsilon}_{ii}^{\frac{1-n_i}{n_i}} exp\left(\frac{E_i + PV_i}{nRT}\right)$$

, where i stands for dislocation or diffusion creep. The effective viscosity will be:

$$\eta_{eff} = \frac{\eta_{diff} * \eta_{disl}}{\eta_{diff} + \eta_{disl}}$$

Table SI-1 – Rheology parameters of the subduction model.

	Overriding crust	Continental crust	Weak crust	Weak lithosphere	Upper mantle	Lower mantle
$A_{disl}(Pa^{-n}s^{-1})$	8.57e-28	8.57e-28	8.57e-28	6.51e-15	6.51e-15	6.51e-16
n_{disl}	4	4	4	3.8	3.5	3.5
$E_{disl}\ (kJ/mol)$	223	223	223	440	530	530
$V_{disl}(m^3/mol)$	18e-6	18e-6	18e-6	18e-6	18e-6	18e-6
$A_{diff}(m^m/Pas)$	8.88e-15	8.88e-15	8.88e-15	8.88e-15	8.88e-15	8.88e-15
$E_{diff}\ (kJmol^{-1})$	375	375	375	335	335	355
$V_{diff}(m^3/mol)$	6e-6	6e-6	6e-6	6e-6	6e-6	
Angle of internal friction (°)	10	1	5	10	15	15
Cohesion (Pa)	10e6	1e4	1e4	10e6	20e6	20e6
Density (kg/m^3)	3300	3399	3300	3200	3200	3200

2. Rotation from the model reference frame to the CPO reference frame and back

Olivine single crystals have an orthorhombic structure, and thus it is expected that the viscosity tensor for a single crystal olivine will have orthotropic symmetry with 9 independent components in the CPO reference frame. In olivine aggregates with multiple single crystals with different orientations, the average viscosity tensor is expected to have a lower symmetry, which means that the viscosity tensor of olivine in our geodynamic model will have monoclinic symmetry in the macroscopic reference frame.

The constitutive equation that relates stress and strain rate utilizes a fourth-rank anisotropic viscosity tensor such that: $\sigma_{kl} = \eta_{ijkl} * \dot{\varepsilon}_{ij}$. Here the viscosity tensor η_{ijkl} has 81 independent components. For an olivine aggregate with monoclinic symmetry, η_{ijkl} has 21 independent components in the macroscopic model reference frame. To use Hill's parameters for the anisotropic viscosity tensor (Signorelli et al., 2021), we need to rotate the model into the mean CPO reference frame, where we assume an orthotropic symmetry.

To compute the rotation matrix (R_{CPO}) between the model and the CPO reference frame, we first compute the mean orientation of the a-, b-, and c- axes of olivine by taking the eigenvalues and eigenvectors of the orientation matrices for each axis. This method is

equivalent to the Bingham average computation as in ASPECT described by Fraters and Billen (2021). We construct R_{CPO} from the eigenvectors with the largest associated eigenvalues for each axis (a, b, and c axis) of the olivine texture, which gives:

$$R_{CPO} = \begin{bmatrix} max\_eigenvector\_a\_axis(1) & max\_eigenvector\_b\_axis(1) & max\_eigenvector\_c\_axis(1) \\ max\_eigenvector\_a\_axis(2) & max\_eigenvector\_b\_axis(2) & max\_eigenvector\_c\_axis(2) \\ max\_eigenvector\_a\_axis(3) & max\_eigenvector\_b\_axis(3) & max\_eigenvector\_c\_axis(3) \end{bmatrix}$$

The constitutive equation (equation 1) from the main text in the CPO reference frame is:

$\dot{\varepsilon}_{CPO} = \gamma \, \mathrm{J} \, (\sigma_{CPO})^{n-1} \mathrm{A} : (R'_{CPO} : \sigma_{mod} : R_{CPO})$,

where σ_{mod} is the stress in model reference frame. To find the strain rate in model reference frame, we first need to rotate the stress in the model reference frame into the CPO reference frame in order to calculate anisotropic viscosity tensor. Then we rotate the fluidity tensor back into model reference frame. Thus, the constitutive equation that we use in model reference frame is:

$$\dot{\varepsilon}_{mod} = (R_{CPO\_K} : (\gamma \, \mathrm{J} \, (R'_{CPO} : \sigma_{mod} : R_{CPO})^{n-1} \mathrm{A}) : R'_{CPO\_K}) : \sigma_{mod}$$

where R_{CPO_K} is the rotation matrix that rotates the fourth-rank tensor in Kelvin notation from the CPO reference frame to the model reference frame constructed from R_{CPO} (Mehrabadi & Cowin, 1990):

$$R_{CPO\_K} = \begin{bmatrix} R_{11}^2 & R_{12}^2 & R_{12}^2 & \sqrt{2}R_{12}R_{13} & \sqrt{2}R_{11}R_{13} & \sqrt{2}R_{11}R_{12} \\ R_{21}^2 & R_{22}^2 & R_{23}^2 & \sqrt{2}R_{22}R_{23} & \sqrt{2}R_{21}R_{23} & \sqrt{2}R_{21}R_{22} \\ R_{31}^2 & R_{32}^2 & R_{33}^2 & \sqrt{2}R_{32}R_{33} & \sqrt{2}R_{31}R_{33} & \sqrt{2}R_{31}R_{32} \\ \sqrt{2}R_{21}R_{31} & \sqrt{2}R_{22}R_{32} & \sqrt{2}R_{23}R_{33} & R_{22}R_{33}+R_{23}R_{32} & R_{21}R_{33}+R_{23}R_{31} & R_{21}R_{32}+R_{22}R_{31} \\ \sqrt{2}R_{11}R_{31} & \sqrt{2}R_{12}R_{32} & \sqrt{2}R_{13}R_{33} & R_{12}R_{33}+R_{13}R_{32} & R_{11}R_{33}+R_{13}R_{31} & R_{11}R_{32}+R_{12}R_{31} \\ \sqrt{2}R_{11}R_{21} & \sqrt{2}R_{12}R_{22} & \sqrt{2}R_{13}R_{23} & R_{12}R_{23}+R_{13}R_{22} & R_{11}R_{23}+R_{13}R_{21} & R_{11}R_{22}+R_{12}R_{21} \end{bmatrix}$$

, where matrix components R_{ij} in R_{CPO_K} come from the matrix R_{CPO} above.

3. Movement towards the y-direction for the mantle wedge particle

For the MDM+AV model, we see a transition from a girdle-like texture to a point-like texture in Figure 7a, from time step 13 to 20. During this period, the maximum is moving towards the y-direction in the MDM+AV model, but not in the other models (Figure SI-1). From the velocity gradient tensors in Table SI-2 from time step 13 to 20, we can see that this movement can be explained by the D_{23} component of the velocity gradient tensor, where D_{23} for MDM+AV (normalized by D_{11}) is more than ten times larger than D_{23} for ASPECT (D-Rex). D_{23} for MDM+AV also follows an increasing trend during these time steps, showing that the y-direction movement is accelerating as the texture re-aligns. Since the velocity gradient of MDM+AV is scaled using the anisotropic viscosity associated with the texture (specifically, the ratio between the ASPECT strain rate and the MDM+AV strain rate, which is computed using the fluidity tensor associated with the texture), we suggest that the y-direction movement reflects the effect of AV.

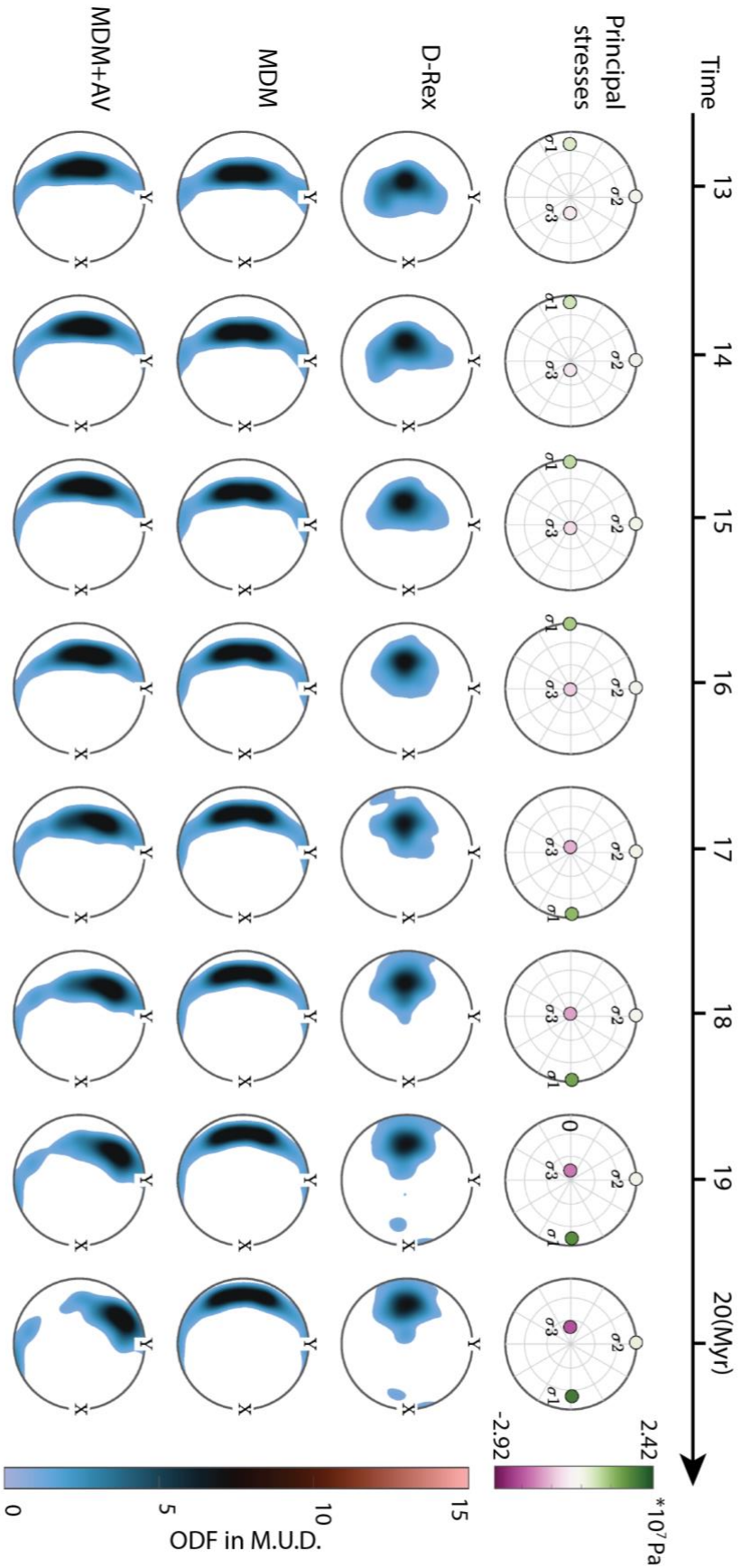

Figure SI-1. Principal stresses from the deviatoric stress tensors and pole figures of the olivine a-axis from time step 13 to 20.

Table SI-2. Velocity gradient tensors (D) from ASPECT as computed using D-Rex (left column) and MDM+AV (right column). All values are normalized by the D_{11} component.

velocity gradient (ASPECT)			velocity gradient (MDM+AV)		
Time step 13					
1	0.002422	0.23984	1	0.000445	0.238886
0.037869	0.005931	0.026333	0.006959	0.024527	0.461423
-1.04064	-0.00677	-0.92524	-1.0365	-0.1187	-1.02453
Time step 14					
1	0.003443	0.5303	1	0.012006	0.454329
0.030515	0.005931	0.028704	0.106414	0.037844	0.33671
-0.82578	-0.00676	-1.03117	-0.70748	-0.07932	-1.03784
Time step 15					
1	0.003213	0.645622	1	0.022698	1.886914
0.027471	0.005215	0.026579	0.194041	-0.18287	0.173842
-0.70757	-0.00501	-0.93244	-2.06796	-0.03275	-0.81713
Time step 16					
1	0.004321	1.073065	1	-0.01835	1.764435
0.025302	0.005636	0.034418	-0.10747	0.446245	0.737777
-0.57036	-0.00474	-1.08099	-0.93784	-0.1015	-1.44625
Time step 17					
1	0.005223	0.605768	1	0.033665	0.523586
0.024695	0.006895	0.024501	0.159165	-0.05582	0.706111
-0.40411	-0.005	-0.74474	-0.34928	-0.14409	-0.94418
Time step 18					
1	0.005523	1.114716	1	0.041765	1.236822
0.023648	0.008606	0.039695	0.17884	0.13594	0.959895
-0.19413	-0.00445	-1.0466	-0.21539	-0.10772	-1.13594
Time step 19					
1	0.007114	2.186298	1	0.023572	2.766975
0.026023	0.011838	0.071271	0.086232	0.55458	1.500466
0.034801	-0.00468	-1.42407	0.044044	-0.09851	-1.55458
Time step 20					
1	0.009567	1.48098	1	0.066254	1.812826
0.025284	0.017826	0.064265	0.175092	0.351911	1.509836
0.429204	-0.00531	-1.24557	0.525376	-0.1247	-1.35191

References

Fraters, M. R. T., & Billen, M. I. (2021). On the Implementation and Usability of Crystal Preferred Orientation Evolution in Geodynamic Modeling. *Geochemistry, Geophysics, Geosystems*, *22*(10). https://doi.org/10.1029/2021GC009846

Mehrabadi, M. M., & Cowin, S. C. (1990). Eigentensors of linear anisotropic elastic materials. *The Quarterly Journal of Mechanics and Applied Mathematics*, *43*(1), 15–41. https://doi.org/10.1093/qjmam/43.1.15

Signorelli, J., Hassani, R., Tommasi, A., & Mameri, L. (2021). An effective parameterization of texture-induced viscous anisotropy in orthotropic materials with application for modeling geodynamical flows. *Journal of Theoretical, Computational and Applied Mechanics*, 6737. https://doi.org/10.46298/jtcam.6737